Research Journal of Applied Sciences, Engineering and Technology 6(17): 3125-3136, 2013
ISSN: 2040-7459; e-ISSN: 2040-7467

Submitted: January 12, 2013 Accepted: February 07, 2013 Published: September 20, 2013

The Effect of Apertures Position on Shielding Effectiveness of Metallic Enclosures based on Modal Method of Moments

[1, 2]Chao Zhou and [1]Ling Tong
[1]School of Automation Engineering, University of Electronic Science and Technology of China, Chengdu 610054, China
[2]Aviation Engineering Institute, Civil Aviation Flight University of China, Guanghan Sichuan 618307, China

Abstract: In this study, an effective numerical method suitable for determination of electric field Shielding Effectiveness (SE) of rectangular enclosure with multiple rectangular apertures is presented. Assuming appropriate electric field distribution on the aperture, Electromagnetic fields inside the enclosure are determined using rectangular cavity Green's function. Electromagnetic fields outside the enclosure and scattered due to the aperture are obtained using the free space Green's function. Matching the tangential magnetic field across the apertures, the integral equation with aperture fields as unknown variables is obtained. The integral equation is solved for unknown aperture fields using the Method of Moments. From the aperture fields the electromagnetic SE of the rectangular enclosure is determined. The numerical results of the proposed technique are in very good agreement with data available in the literature and experimental results. It is shown that apertures' position and shape, aperture' number, polarization have noticeable effect on the electric field SE.

Keywords: Apertures, green's function, MoM, rectangular enclosure, Shielding Effectiveness (SE)

INTRODUCTION

Most aircraft used a series of cables, chains, cranks and mechanical mechanisms to operate the systems which gave the aircraft its ability to fly in the past. Nowadays many mechanical devices have been replaced or augmented with avionics. Electronic devices have increasingly been designed and used for flight critical aircraft control systems, because of their ability to accurately control complex functions and increase reliability. Electronic circuits, however, not only respond to their internal electrical signal flow, but may respond to any input which can couple into the wire bundles, wires, IC leads and electrical junctions. The Electromagnetic Environment (EME) is one of these inputs that has access to all these electronic circuits and may result in disabling effects called Electromagnetic Interference (EMI). The aircraft skin and structure have also evolved. The classic aircraft is made of aluminum and titanium structure with an aluminum skin. Modern technology and the desire to develop more efficient aircraft have driven the introduction of carbon-epoxy structure, carbon-epoxy skins and aramid fiber-epoxy skins in civil aircraft. Aluminum may be a good EM shield against High Intensity Radiated Field (HIRF) and hence electronic circuits are provided inherent protection. However, some composites are poor EM shields, causing HIRF to irradiate the electronic systems on such aircraft with relatively little attenuation. So electromagnetic shielding is an important technique in Electromagnetic Compatibility (EMC). It can restrain electromagnetic energy radiation and prevent the electromagnetic interference effectively.

Nowadays metallic shielding enclosures are frequently employed to suppress its directive radiation effects. Unfortunately, in practical applications, the integrity of these metallic enclosures is often compromised by all kinds of apertures that are used to accommodate visibility, ventilation or access to interior components, such as input and output connections, heat dispersion panels, control panels, visual-access windows, etc. What is more, those openings allow exterior electromagnetic energy to penetrate to the inside space, where they may couple onto Printed Circuit Boards (PCBs), then cause the inner field resonance and the shielding performance being degraded. So it is very important to know the EM Shielding Effectiveness (SE) of shielding enclosures in the presence of these apertures. The EM SE study may also help in locating these apertures at proper places to reduce the EM emission or improving the immunity of electronic components present inside the metallic enclosure.

Several analytical and numerical techniques to estimate SE of metallic enclosures with apertures have been suggested in past years. However, each technique has advantages and disadvantages with respect to other techniques. Pure analytical formulations even though

Corresponding Author: Chao Zhou, Aviation Engineering Institute, Civil Aviation Flight University of China, Guanghan Sichuan 618307, China

provide a much faster means of calculating SE are based on various simplifying assumptions whose validity may be questionable at high frequencies.

Robinson *et al*. (1996, 1998) introduced a very simple analytical method based on transmission line model. However, this approach is limited by the assumption of thin apertures, simple geometries, negligible mutual coupling between apertures and fields can be calculated only at points in front of the aperture. The transmission line model was later extended to include higher order cavity modes (Belokour *et al*., 2001) and the effects of loading due to electrical circuits within the enclosure (Thomas *et al*., 1999).

In addition, some efficient and reliable numerical techniques for the electromagnetic analysis and many numerical tools have been applied to the analysis of shielding effectiveness, such as Finite Difference Time Domain (FDTD) (Jiao *et al*., 2006; Li *et al*., 2000), Finite Element Method (FEM) (Benhassine *at al*., 2002; Carpes *et al*., 2002), method of moments (MoM) (Wallyn *et al*., 2002; Wu *et al*., 2011), Transmission Line Matrix (TLM) (Podlozny *et al*., 2002; Attari and Barkeshli, 2002) and hybrid method (Wu *et al*., 2010) are utilized with good accuracy over a broad frequency band at the cost of large amount of computer memory and CPU time.

Deshpande introduced a moment method technique (modal MoM) using entire domain basis functions to represent apertures fields and therefore the magnetic currents on the apertures, which can evaluates the SE of a zero thickness enclosure exposed to a normally incident plane wave accurately at the center inside enclosure (Deshpande, 2000). This method has been further modified for obliquely polarimetric incident plane wave (Ali *et al*., 2005; Jayasree *et al*., 2010) and for finite wall thickness (Dehkhoda *et al*., 2009). Nowadays the EM shielding effectiveness has becoming a hot research point in the electromagnetic compatibility area (Bahadorzadeh and Moghaddasi, 2008; Robertson *et al*., 2008; Faghihi and Heydari, 2009; Koledintseva *et al*., 2009; Wang and Koh, 2004; Hussein, 2007; Morari *et al*., 2011; Kim *et al*., 2008; Bahadorzadeh and Moghaddasi, 2008).

In the majority of the aforementioned methods, there are few studies on the influence of apertures' position on shielding effectiveness of metallic enclosures with apertures. In this study the modal MoM solution is formulated, the apertures are replaced by equivalent magnetic current sources, employing the surface equivalence principle and boundary conditions at each end of the aperture, matching the tangential electromagnetic fields across the apertures, coupled integral differential equations with the magnetic currents at the apertures as unknown variables are obtained. The coupled integral differential equation in conjunction with the method of moment is then solved for unknown magnetic current amplitudes. The electric field SE has been calculated at many points inside the enclosure with multiple rectangular apertures sat different places. The electric field SE due to horizontal as well as vertical polarizied incident fields is also studied. A very good agreement among the results of the proposed technique, results available in the literature and experimental results is observed. It is shown that aperture position has noticeable effect to the electric field SE, especial for single aperture case.

ELECTROMAGNETIC PROBLEM AND THE FORMULATION OF MODAL MoM

The shielding effectiveness of an enclosure is defined as:

$$\text{SE (dB)} = -20\log\left(\frac{|\boldsymbol{E}_{\text{int}}|}{|\boldsymbol{E}_{\text{ext}}|}\right) \quad (1)$$

where,

E_{int} : The electric field at a given point inside the enclosure

E_{ext} : The electric field at the same point in the absence of the enclosure

Therefore, the problem of estimation of shielding effectiveness is essentially the problem of calculating the cavity fields excited by a plane wave incident from free space upon the shielding enclosure.

Figure 1 shows a rectangular enclosure with rectangular apertures exposed to a normal incident plane wave. The dimensions of the cavity are $a \times b \times c$. There are r number of apertures and the dimensions of the rth aperture are $L_r \times W_r$. The orientation of the reference axes is also shown with the origin at the lower right corner of the front wall.

Apertures fields and equivalent magnetic currents: In the Modal MoM formulation, we assume that the apertures are relatively small compared to the walls in which they are located and are placed far enough away from the edges of the enclosure. In addition, the edge diffracted fields are neglected. These assumptions enable us to use image theory and equivalence principles, using the surface equivalence principle, the apertures both internal (Region II) and external (Region I) to the enclosure can be replaced by equivalent magnetic currents of:

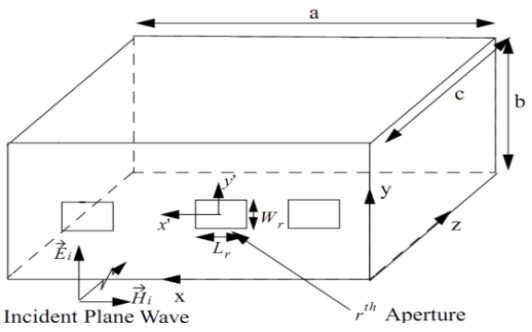

Fig. 1: Geometry of rectangular enclosure with rectangular apertures exposed to a normal incident plane wav

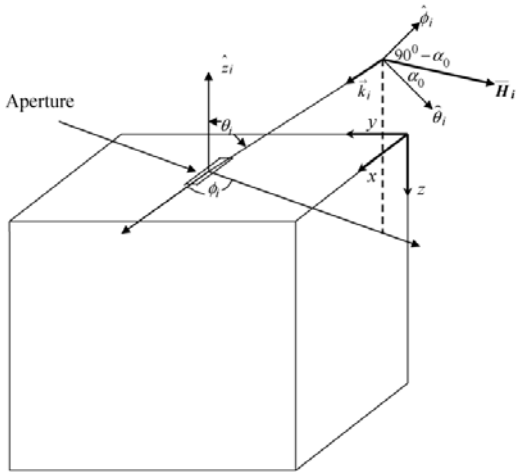

Fig. 2: Definition of angle of incidence and polarization

$$M = n \times E_{apt} \tag{2}$$

where, E_{apt} is the tangential electric field induced on the apertures and n is the aperture normal vector:

$$E_{apt}(\text{z} = 0) = \sum_{r=1}^{R} \begin{bmatrix} \hat{y} \sum_p \sum_q U_{rpq} \sin\left(\frac{p\pi}{L_r}\left(\frac{L_r}{2} + x - x_{cr}\right)\right) \\ \times \cos\left(\frac{q\pi}{W_r}\left(\frac{W_r}{2} + y - y_{cr}\right)\right) \\ + \hat{x} \sum_p \sum_q V_{rpq} \cos\left(\frac{p\pi}{L_r}\left(\frac{L_r}{2} + x - x_{cr}\right)\right) \\ \times \sin\left(\frac{q\pi}{W_r}\left(\frac{W_r}{2} + y - y_{cr}\right)\right) \end{bmatrix} \tag{3}$$

where, U_{rpq} and V_{rpq} are the unknown amplitudes of the pq^{th} mode of magnetic current on the outer of the r^{th} aperture, $U_{rpq} \neq 0$ and $V_{rpq} \neq 0$ for $x_{cr} - \frac{L_r}{2} \leq x \leq x_{cr} + \frac{L_r}{2}$, $y_{cr} - \frac{W_r}{2} \leq y \leq y_{cr} + \frac{W_r}{2}$ and $U_{rpq} = V_{rpq} = 0$ otherwise. L_r *and* W_r are the length and width of r^{th} aperture, x_{cr} and y_{cr} are center coordinates of the r^{th} aperture. $\hat{x}$, $\hat{y}$ are the unit vectors in x, y directions. The unknown amplitudes U_{rpq}, V_{rpq} are determined by setting up coupled integral equations.

Using the equivalence principle, the equivalent magnetic currents are:

$$M_{apt} = n_1 \times E_{apt} = -\hat{z} \times E_{apt} \ (\text{z} = 0)$$

$$= \sum_{r=1}^{R} \left[\hat{x} \sum_p \sum_q U_{rpq} \Psi_r - \hat{y} \sum_p \sum_q V_{rpq} \Phi_r\right] = \sum_{r=1}^{R} M_{r1} \tag{4}$$

where,

$$\Psi_r = \sin\left(\frac{p\pi}{L_r}\left(\frac{L_r}{2} + x - x_{cr}\right)\right) \times \cos\left(\frac{q\pi}{W_r}\left(\frac{W_r}{2} + y - y_{cr}\right)\right) \tag{5}$$

$$\Phi_r = \cos\left(\frac{p\pi}{L_r}\left(\frac{L_r}{2} + x - x_{cr}\right)\right) \times \sin\left(\frac{q\pi}{W_r}\left(\frac{W_r}{2} + y - y_{cr}\right)\right) \tag{6}$$

Electromagnetic field due to incident wave: Figure 2 is the definition of incidence and polarization angles. The incident time harmonic plane wave illuminating the rectangular apertures on the cavity can be written as:

$$H_i = (\hat{\theta}_i H_{\theta_i} + \hat{\emptyset}_i H_{\emptyset_i}) e^{-jk_i \cdot r} =$$

$$(\hat{\theta}_i H_i cos\alpha_0 + \hat{\emptyset}_i H_i sin\alpha_0) e^{-jk_i \cdot r}) \tag{7}$$

where,

$k_i \cdot r = k_0 \sin\theta_i (x cos\emptyset_i + y sin\emptyset_i) + z k_0 cos\theta_i$
k_0 = Free space wave number
$\theta_i, \emptyset_i$ = Angles of incident plane wave
α_0 = Polarization of the incident plane wave

From Eq. (7), the x-, y- and z-components of the incident magnetic field may be written, respectively as:

$$H_{xi} = H_{\theta_i} \cos\theta_i \cos\emptyset_i - H_{\emptyset_i} \sin\emptyset_i \tag{8}$$

$$H_{yi} = H_{\theta_i} \cos\theta_i \sin\emptyset_i - H_{\emptyset_i} \cos\emptyset_i \tag{9}$$

$$H_{zi} = -H_{\theta_i} \sin\theta_i \tag{10}$$

For normal incidence, with $\alpha_0 = 0, \theta_i = 0$ and $\emptyset_i = 0$, the incident field in the z = 0 is given by $H_{xi} = H_i, H_{yi} = 0$ *and* H_{zi}=0.

Electromagnetic field outside enclosure: Consider the aperture on the z = 0 plane, the scattered EM field outside due to the rth aperture can be determined by solving electric vector potential:

$$E = -\frac{1}{\varepsilon_0} \nabla \times F \tag{11}$$

$$H = -\frac{j\omega}{k_0^2} (k_0^2 F + \nabla \nabla \cdot F) \tag{12}$$

where the electric vector potential F is given by:

$$F = \frac{\varepsilon_0}{4\pi} \iint_{apt} 2M_r \frac{e^{-jk_0|r-r'|}}{r-r'} ds \tag{13}$$

Superposition of the scattered electromagnetic field due to all apertures on the z =0 plane gives the total scattered field as (Deshpande, 2000):

$$H_x^1 = \sum_{r=1}^{R} \sum_p \sum_q \frac{\omega \varepsilon_0}{4\pi^2 k_0^2} (U_{rpq} \int_{-\infty}^{\infty} \int_{-\infty}^{\infty} e^{-jk_z|z-z'|} \psi_{rpqy}$$

$$\times \frac{k_0^2 - k_x^2}{k_z} e^{jk_x x + jk_y y} dk_x dk_y - V_{rpq} \int_{-\infty}^{\infty} \int_{-\infty}^{\infty} e^{-jk_z|z-z'|}$$

$$\times \phi_{rpqy} \frac{-k_x k_y}{k_z} e^{jk_x x + jk_y y} dk_x dk_y) \tag{14}$$

$$H_y^{\mathrm{I}} = \sum_{r=1}^{R}\sum_p\sum_q \frac{-\omega\varepsilon_0}{4\pi^2 k_0^2}\Big(V_{rpq}\int_{-\infty}^{\infty}\int_{-\infty}^{\infty} e^{-jk_z|z-z'|}\,\phi_{rpqy} \times \frac{k_0^2-k_y^2}{k_z} e^{jk_x x+jk_y y}dk_x dk_y - U_{rpq}\int_{-\infty}^{\infty}\int_{-\infty}^{\infty} e^{-jk_z|z-z'|} \psi_{rpqy}\frac{-k_x k_y}{k_z} e^{jk_x x+jk_y y}dk_x dk_y\Big) \quad (15)$$

$$H_z^{\mathrm{I}} = \sum_{r=1}^{R}\sum_p\sum_q \frac{-\omega\varepsilon_0}{4\pi^2 k_0^2}\Big(\int_{-\infty}^{\infty}\int_{-\infty}^{\infty} e^{-jk_z|z-z'|}\big(U_{rpq}\psi_{rpqy}k_x - V_{rpq}\,\phi_{rpqy}k_y\big)e^{jk_x x+jk_y y}dk_x dk_y \quad (16)$$

In expressions (14) - (16) ϕ_{rpqy} is the Fourier transform of Φ_{rpqy} and ψ_{rpqy} is the Fourier transform of Ψ_{rpqx}.

Electromagnetic field inside enclosure: The equivalent magnetic currents, present on the apertures of the enclosure, radiate electromagnetic fields inside the enclosure. The total electromagnetic field at any point inside enclosure is obtained by a superposition of fields due to each equivalent magnetic current source. Considering the x-component of the magnetic current and using dyadic Green's function, the total magnetic field inside the enclosure is then obtained from Deshpande (2000) as:

$$H_x^{\mathrm{IIx0}} = \frac{-j\omega}{k_0^2}\sum_{r=1}^{R}\sum_{p,q} U_{rpq}\sum_{m,n}^{\infty}\frac{-\varepsilon_0}{k_I}\frac{\varepsilon_{0m}\varepsilon_{0n}}{ab\sin(k_I c)} \times\left(k_0^2-\left(\frac{\mathrm{m}\pi}{\mathrm{a}}\right)^2\right)\sin\left(\frac{m\pi x}{a}\right) \times\cos(\frac{n\pi y}{b})\cos(k_I(z-c))I_{rpq\mathrm{mn}x} \quad (17)$$

$$H_y^{\mathrm{IIx0}} = \frac{-j\omega}{k_0^2}\sum_{r=1}^{R}\sum_{p,q} U_{rpq}\sum_{m,n}^{\infty}\frac{-\varepsilon_0}{k_I}\frac{\varepsilon_{0m}\varepsilon_{0n}}{ab\sin(k_I c)} \times\frac{m\pi}{a}(-\frac{n\pi}{b})\cos\left(\frac{m\pi x}{a}\right) \times\sin\left(\frac{n\pi y}{b}\right)\cos\big(k_I(z-c)\big)I_{rpq\mathrm{mn}x} \quad (18)$$

$$H_z^{\mathrm{IIx0}} = \frac{-j\omega}{k_0^2}\sum_{r=1}^{R}\sum_{p,q} U_{rpq}\sum_{m,n}^{\infty}\frac{-\varepsilon_0}{k_I}\frac{\varepsilon_{0m}\varepsilon_{0n}}{ab\sin(k_I c)} \times\frac{m\pi}{a}(-k_I)\cos\left(\frac{m\pi x}{a}\right) \times\cos\left(\frac{n\pi y}{b}\right)\sin\big(k_I(z-c)\big)I_{rpq\mathrm{mn}x} \quad (19)$$

In (17)-(19):

$$I_{rpq\mathrm{mn}x} = \iint_q \Psi_{rpqx}(x',y')\sin\left(\frac{\mathrm{m}\pi x'}{\mathrm{a}}\right)\cos(\frac{n\pi y'}{b})dx'dy'$$

Likewise, considering the y-component of the magnetic current and using the proper boundary conditions, the total magnetic field inside the enclosure is then obtained from Deshpande (2000) as:

$$H_x^{\mathrm{IIy0}} = \frac{-j\omega}{k_0^2}\sum_{r=1}^{R}\sum_{p,q} -V_{rpq}\sum_{m,n}^{\infty}\frac{-\varepsilon_0}{k_I}\frac{\varepsilon_{0m}\varepsilon_{0n}}{ab\sin(k_I c)} \times(-\frac{m\pi}{a})\frac{n\pi}{b}\sin\left(\frac{m\pi x}{a}\right)\cos(\frac{n\pi y}{b}) \times\cos(k_{\mathrm{I}_r}(z-c))I_{rpq\mathrm{mn}y} \quad (20)$$

$$H_y^{\mathrm{IIy0}} = \frac{-j\omega}{k_0^2}\sum_{r=1}^{R}\sum_{p,q} -V_{rpq}\sum_{m,n}^{\infty}\frac{-\varepsilon_0}{k_I}\frac{\varepsilon_{0m}\varepsilon_{0n}}{ab\sin(k_I c)} \times\left(k_0^2-\left(\frac{n\pi}{b}\right)^2\right)\cos\left(\frac{m\pi x}{a}\right) \times\sin\left(\frac{n\pi y}{b}\right)\cos\big(k_I(z-c)\big)I_{rpq\mathrm{mn}y} \quad (21)$$

$$H_z^{\mathrm{IIy0}} = \frac{-j\omega}{k_0^2}\sum_{r=1}^{R}\sum_{p,q} -V_{rpq}\sum_{m,n}^{\infty}\frac{-\varepsilon_0}{k_I}\frac{\varepsilon_{0m}\varepsilon_{0n}}{ab\sin(k_I c)} \times\frac{n\pi}{b}(-k_I)\cos\left(\frac{m\pi x}{a}\right) \times\cos(\frac{n\pi y}{b})\sin(k_I(z-c))I_{rpq\mathrm{mn}y} \quad (22)$$

In (20)-(22):

$$I_{rpq\mathrm{mn}y} = \iint_q \Phi_{rpqy}(x',y')\cos\left(\frac{\mathrm{m}\pi x'}{\mathrm{a}}\right)\sin(\frac{n\pi y'}{b})dx'dy'$$

For a unique solution the electromagnetic fields in various regions satisfy continuity conditions over their common surfaces. The tangential electric fields over the apertures are continuous. The tangential magnetic over the apertures must also be continuous, thus yielding coupled integral equations with the magnetic currents as known variables. The coupled integral equation in conjunction with the method of moments can be solved for the amplitudes of magnetic currents.

Derivation of integral equation: The total tangential fields inside the cavity from apertures are written as:

$$\mathrm{H_x^{II}} = \mathrm{H_x^{IIx0}} + \mathrm{H_x^{IIy0}} \quad (23)$$

$$H_y^{II} = H_y^{IIx0} + H_y^{IIy0} \quad (24)$$

Applying the continuity of tangential magnetic field on the z = 0 plane yields:

$$H_x^{I}|_{z=0} + H_{xi}|_{z=0} = H_x^{\mathrm{II}}|_{z=0} \quad (25)$$

$$H_y^I|_{z=0}+H_{yi}|_{z=0}= H_y^{II}|_{z=0} \quad (26)$$

Now selecting $\Psi_{r'p'q'x}$ as a testing function and use of Galerkin's method reduces the (25) to:

$$I_{r'p'q'xi} = \sum_{r=1}^{R}\sum_{p,q}(U_{rpq}Y_{rpqr'p'q'}^{x1x1} + V_{rpq}Y_{rpqr'p'q'}^{x1y1}) \quad (27)$$

where,

$$Y_{rpqr'p'q'}^{x1x1}=\frac{-j\omega}{k_0^2}\sum_{m,n=0}^{\infty}\frac{-\varepsilon_0}{k_I}\frac{\varepsilon_{0m}\varepsilon_{0n}}{ab\sin(k_Ic)}$$

$$\times(k_0^2-\left(\frac{m\pi}{a}\right)^2)\cos(k_Ic)I_{rpqmnx}I_{r'p'q'mnx}$$

$$+\frac{\omega\varepsilon_0}{4\pi^2k_0^2}\int_{-\infty}^{+\infty}\int_{-\infty}^{+\infty}\Psi_{rpqx}\Psi_{r'p'q'x}^{*}\frac{k_0^2-k_x^2}{k_z}dk_xdk_y \quad (28)$$

$$Y_{rpqr'p'q'}^{x1y1}=\frac{j\omega}{k_0^2}\sum_{m,n=0}^{\infty}\frac{-\varepsilon_0}{k_I}\frac{\varepsilon_{0m}\varepsilon_{0n}}{ab\sin(k_Ic)}\left(\frac{-m\pi}{a}\right)\left(\frac{n\pi}{b}\right)$$

$$\times\cos(k_Ic)\,I_{rpqmny}I_{r'p'q'mnx}$$

$$+\frac{\omega\varepsilon_0}{4\pi^2k_0^2}\int_{-\infty}^{+\infty}\int_{-\infty}^{+\infty}\phi_{rpqy}\,\psi_{r'p'q'x}^{*}\frac{-k_xk_y}{k_z}dk_xdk_y \quad (29)$$

$$I_{r'p'q'xi}=\iint_{r'p'q'}H_{xi}\Psi_{r'p'q'x}\,dxdy \quad (30)$$

Similarly, selecting $-\Phi_{r'p'q'y}$ as a testing function and use of Galerkin's method reduces the (26) to:

$$I_{r'p'q'yi} = \sum_{r=1}^{R}\sum_{p,q}(U_{rpq}Y_{rpqr'p'q'}^{y1x1} + V_{rpq}Y_{rpqr'p'q'}^{y1y1}) \quad (31)$$

where,

$$Y_{rpqr'p'q'}^{y1x1}=\frac{j\omega}{k_0^2}\sum_{m,n=0}^{\infty}\frac{-\varepsilon_0}{k_I}\frac{\varepsilon_{0m}\varepsilon_{0n}}{ab\sin(k_Ic)}\left(\frac{m\pi}{a}\right)\left(-\frac{n\pi}{b}\right)$$

$$\times\cos(k_Ic)I_{rpqmnx}I_{r'p'q'mny}+$$

$$\frac{\omega\varepsilon_0}{4\pi^2k_0^2}\int_{-\infty}^{+\infty}\int_{-\infty}^{+\infty}\psi_{rpqx}\Phi_{r'p'q'y}^{*}\frac{-k_xk_y}{k_z}dk_xdk_y \quad (32)$$

$$Y_{rpqr'p'q'}^{y1y1}=-\frac{j\omega}{k_0^2}\sum_{m,n=0}^{\infty}\frac{-\varepsilon_0}{k_I}\frac{\varepsilon_{0m}\varepsilon_{0n}}{ab\sin(k_Ic)}$$

$$\times\left(k_0^2-\left(\frac{n\pi}{b}\right)^2\right)\cos(k_Ic)I_{rpqmny}I_{r'p'q'mny}$$

$$-\frac{\omega\varepsilon_0}{4\pi^2k_0^2}\int_{-\infty}^{+\infty}\int_{-\infty}^{+\infty}\Phi_{rpqy}\,\Phi_{r'p'q'y}^{*}\frac{(k_0^2-k_x^2)}{k_z}dk_xdk_y \quad (33)$$

$$I_{r'p'q'yi}=\iint_{r'p'q'}H_{yi}\Phi_{r'p'q'x}\,dxdy \quad (34)$$

Equation (27) and (31) can be written in a matrix form as:

$$\begin{bmatrix}Y_{rpqr'p'q'}^{x1x1} & Y_{rpqr'p'q'}^{x1y1}\\ Y_{rpqr'p'q'}^{y1x1} & Y_{rpqr'p'q'}^{y1y1}\end{bmatrix}\begin{bmatrix}U_{rpq}\\ V_{rpq}\end{bmatrix}=\begin{bmatrix}I_{r'p'q'xi}\\ 0\end{bmatrix} \quad (35)$$

The matrix Eq. (35) can be numerically solved for the unknown amplitudes of equivalent magnetic currents induced on the apertures due to given incident field. From the knowledge of these amplitudes electromagnetic field inside as well as outside the enclosure can be obtained.

VALIDATION OF THE PRESENT TECHNIQUE

In this section, for the validation of the presented method, we consider a rectangular enclosure of size ($30 \times 12 \times 30\ cm$) with a rectangular aperture of size (10×0.5 cm) located at the center of the front wall (15 cm, 6 cm, 0), as illustrated in Fig. 3. The enclosure is illuminated by a normal incident plane wave at 0 polarization.

Assuming only expansion mode on the aperture and considering only dominant mode inside the cavity. The shielding effectiveness is calculated at the center of the cavity. Electric field shielding obtained using expression (35) is plotted in Fig. 4 along with the results from Robinson *et al*. (1998). It is observed that the numerical data obtained using the present method agrees well with the earlier published results. Experimental data from Robinson *et al*. (1998) is also reproduced in Fig. 4.

RESULTS AND DISCUSSION

Single aperture case: In next section, we discuss electric field SE results calculated at three different points(x = 15 cm, y = 6 cm, z = 25 cm, 15 and 5 cm, respectively) inside enclosure versus two types of

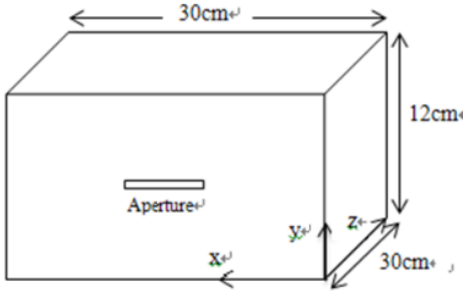

Fig. 3: Geometry of 30× 12 × 30 cm enclosure with a single aperture at (15 cm, 6 cm, 0)

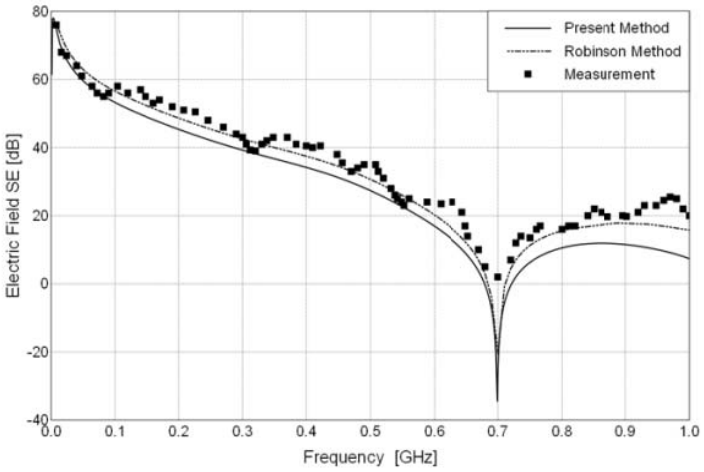

Fig. 4: Electric field SE calculated at the center of 30×12×30 cm enclosure with a 10×0.5 cm aperture located at 15×6 cm in z = 0 plane illuminated by vertical polarized plane wave

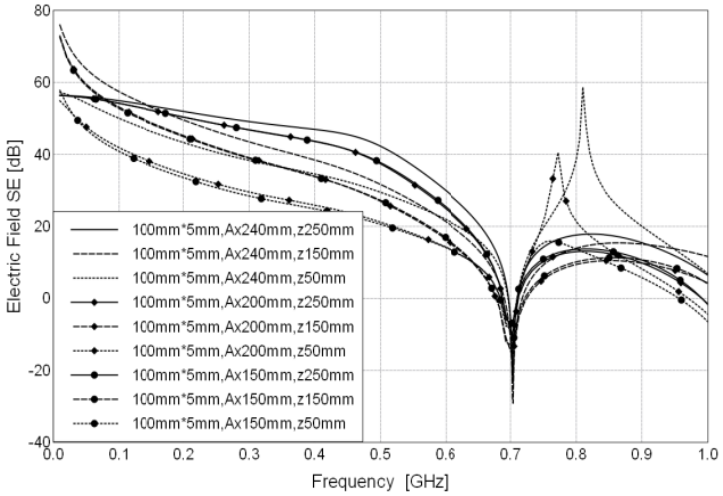

(a) Enclosure illuminated by vertical polarized plane wave

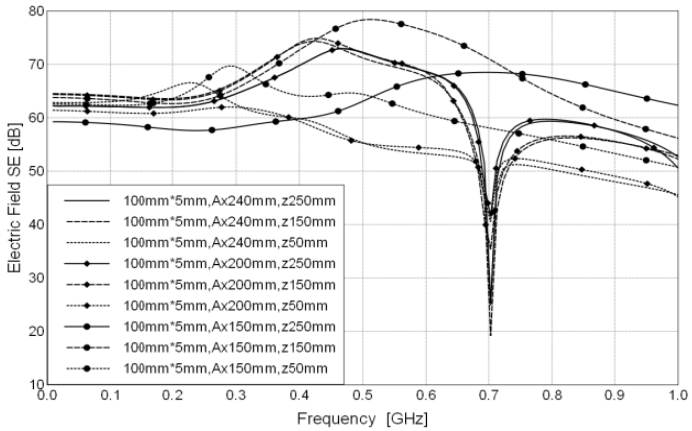

(b) Enclosure illuminated by horizontal polarized plane wave

Fig. 5: Electric field SE versus frequency at three different points (x = 15 cm, y = 6 cm, z = 25 cm, 15 and 5 cm, respectively) inside 30×12×30 cm enclosure with one 10×0.5 cm aperture located at three different places (y = 6 cm, x = 24 cm, 20 and 15 cm, respectively) in z = 0 plane

apertures having same area situated at six different places and illuminated by vertical and horizontal polarized plane wave respectively. We also consider (30×12×30) cm³ enclosure with two types of square aperture of size (10×0.5 cm, 2.23×2.23 cm).

Figure 5 and 6 present the plots of electric field SE versus frequency at three different points(x = 15 cm, y = 6 cm, z = 25, 15 and 5 cm, respectively) inside 30×12×30 cm enclosure with one 10×0.5 cm aperture. In Fig. 5, the aperture located at three different places (y = 6 cm, x = 24 cm, 20 and 15 cm, respectively) in z = 0 plane. In Fig. 6, the aperture located at those places (x = 15 cm, y = 10 cm, 8 and 6 cm, respectively) in z = 0 plane. (a) Enclosure illuminated by vertical polarized plane wave, (b) enclosure illuminated by horizontal polarized plane wave.

In Fig. 5a, we observe a similar behavior for three different places below the first resonance frequency of the cavity, but there are two rapid increase for the calculation point of z = 50 mm because of modal structure of the fields, one up to about 60 dB appear at about 0.82 GHz for the aperture located at x = 24 cm, the other up to about 40 dB appear at about 0.74 GHz for the aperture located at x = 20 cm. We also note that there are little difference for electric field SE of the apertures located at x = 20 cm and x = 15 cm respectively, but for the aperture located at x = 24 cm, the electric field SE are larger than others, especially for the calculation point of z = 5 cm, there are about 10 dB difference.

In Fig. 5b, we note that there are similar trend for apertures located at x = 20 cm and x = 24 cm respectively and the first resonance frequency is also about 0.7 GHz, but for the aperture located at x = 15 cm, it is absolutely different. Comparing (b) with (a), the electric field SE of horizontal has about 15 dB

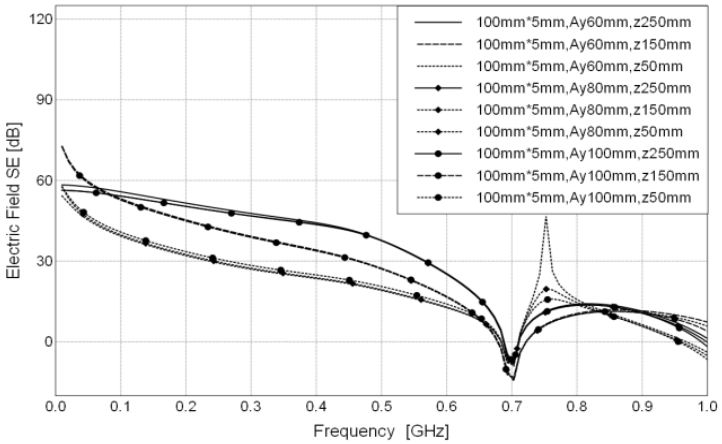

(a) Enclosure illuminated by vertical polarized plane wave

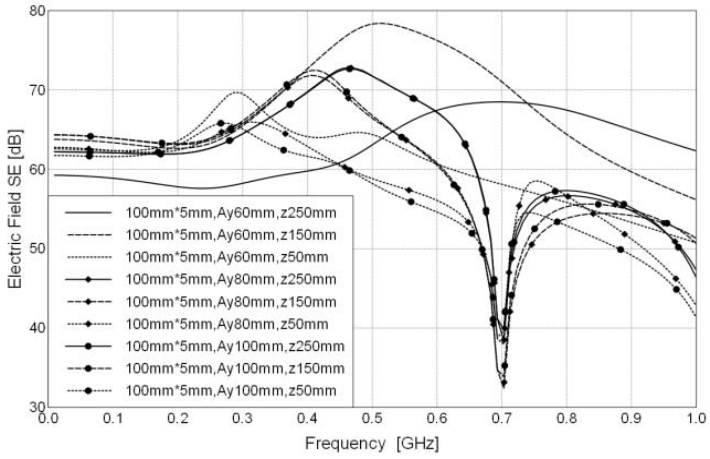

(b) Enclosure illuminated by horizontal polarized plane wave

Fig. 6: Electric field SE versus frequency at three different points (x = 15 cm, y = 6 cm, z = 25 cm, 15 and 5 cm, respectively) inside 30×12×30 cm enclosure with one 10×0.5 cm aperture located at three different places (x = 15 cm, y = 10 cm, 8 and 6 cm, respectively) in z = 0 plane

larger than that of vertical below 0.3 GHz, between 0.4 to 0.6 GHz and 0.75 to 1 GHz, the difference has up to about 35 dB. For the electric field SE of the aperture located at x = 15 cm, it has no resonance below 1 GHz and almost all electric field SE are larger than 60 dB, for the aperture located at x = 15 cm, its SE has even up to about 78 dB at 0.5 GHz. From discussed above, we can safely draw the conclusion that the enclosure with 10×0.5cm aperture has better electric field SE facing the horizontal polarization plane wave, especially for the aperture located at x = 15 cm.

In Fig. 6a, we note that three SE curves have little difference below 1 GHz, which indicates that different y values have little effect on the electric field SE of the enclosure with one 10×0.5 cm aperture illuminated by vertical polarized plane wave. In Fig. 6b, we note that there are similar trend for apertures located at y = 8 cm and y = 10 cm respectively and the first resonance frequency is also about 0.7 GHz. But for the aperture located at y = 6 cm, it is absolutely different, it has no resonance below 1 GHz and almost all electric field SE are larger than 60 dB, the maximum of SE has even up to about 78 dB at 0.5 GHz, which indicate that the place of apertures except for the center of the front wall have minimal effect on the electric field SE.

Figure 7 and 8 present the plots of electric field SE versus frequency at three different points(x = 15 cm, y = 6 cm, z = 25 cm, 15 and 5 cm respectively) inside 30×12×30 cm enclosure with one 2.23×2.23 cm aperture. In Fig. 7, the aperture located at three different places (y = 6 cm, x = 24 cm, 20 and 15 cm respectively) in z = 0 plane. In Fig. 8, the aperture located at those places (x = 15 cm, y =10 cm, 8 and 6 cm respectively) in z = 0 plane. (a) Enclosure illuminated by vertical polarized plane wave, (b) enclosure illuminated by horizontal polarized plane wave.

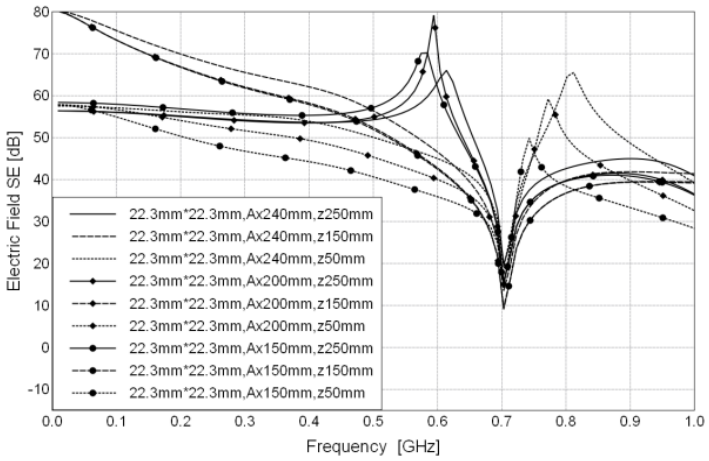

(a) Enclosure illuminated by vertical polarized plane wave

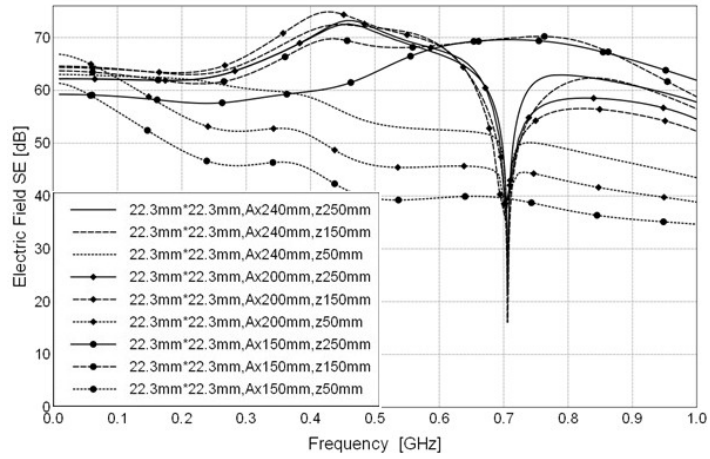

(b) Enclosure illuminated by horizontal polarized plane wave

Fig. 7: Electric field SE versus frequency at three different points (x = 15 cm, y = 6 cm, z = 25 cm, 15 and 5 cm respectively) inside 30×12×30 cm enclosure with one 2.23×2.23 cm aperture located at three different places (y = 6 cm, x = 24, 20 and 15 cm respectively) in z = 0 plane

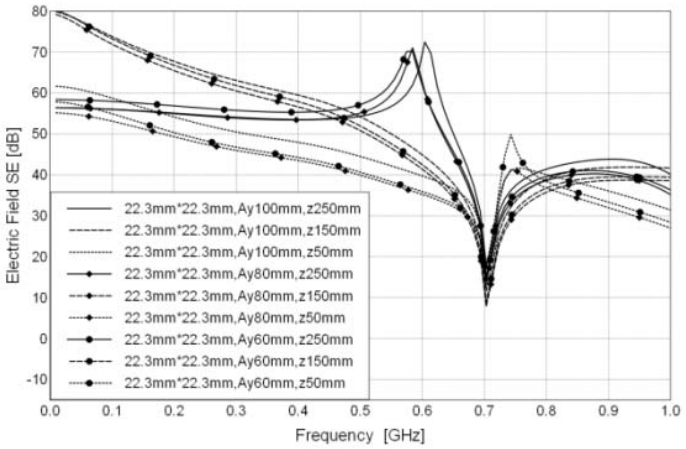

(a) Enclosure illuminated by vertical polarized plane wave

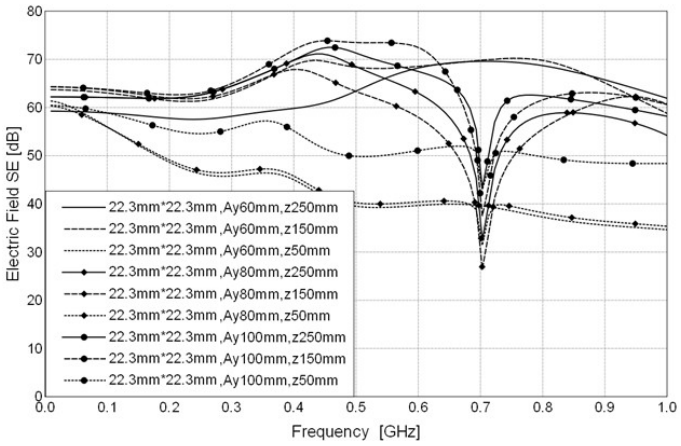

(b) Enclosure illuminated by horizontal polarized plane wave

Fig. 8: Electric field SE versus frequency at three different points (x = 15 cm, y = 6 cm, z = 25 cm, 15 and 5 cm respectively) inside 30×12×30 cm enclosure with one 2.23×2.23 cm aperture located at three different places (x = 15 cm, y = 10, 8 and 6 cm respectively) in z = 0 plane

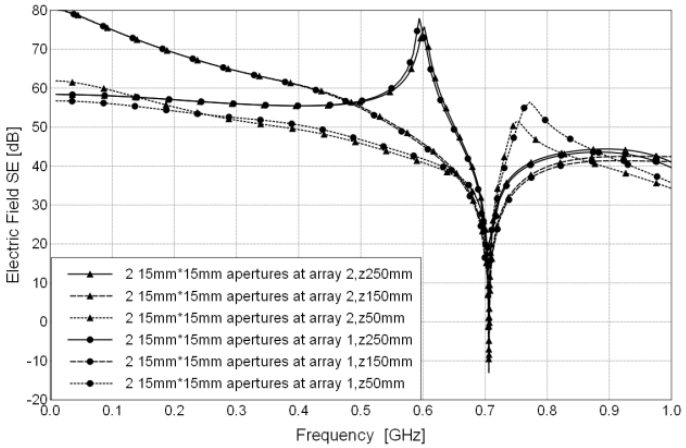

Fig. 9: Electric field SE versus frequency at three different points (x = 15 cm, y = 6cm, z = 25 cm, 15 and 5 cm respectively) inside 30×12×30 cm enclosure with two 1.5×1.5 cm apertures located at array 1 ((150,90,0), (150,30,0)), array 2 ((200, 60, 0), (100, 60, 0)), enclosure illuminated by vertical polarized plane wave

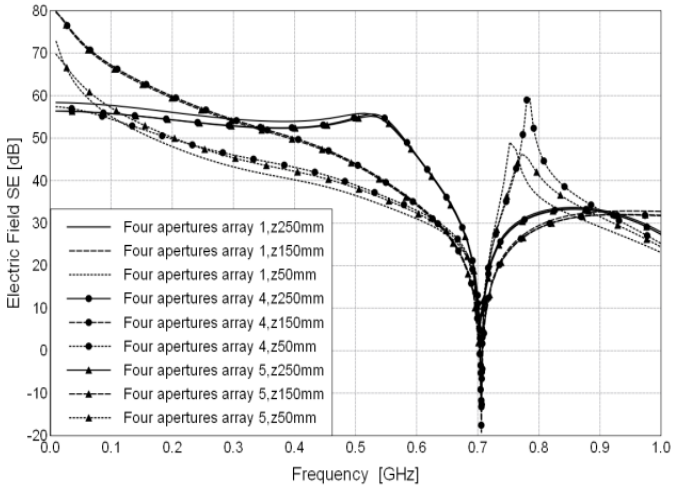

Fig. 10: Electric field SE versus frequency at the center of 30×12×30 cm enclosure with four 2×2 cm apertures located at array 1 ((130, 80, 0), (130, 40, 0), (170, 80, 0), (170, 40, 0)), array 4 ((240, 60, 0), (190, 60, 0), (110, 60, 0), (60, 60, 0)), array 5 ((150, 30, 0), (75, 30, 0), (240, 60, 0), (130, 80, 0)); illuminated by vertical polarized plane wave

Compares Fig. 7 and 8, we find that the enclosure has better electric field SE illuminated by horizontal polarized plane wave and the electric field SE calculated at z = 5 cm are affected more than other points by the places of apertures. Especial for the SE of enclosure with aperture located at x = 15 cm and calculation point at z = 15 cm and z = 25 cm in Fig. 7b, we note that almost all the SE are more than 60 dB, at 0.4 to 0.85 GHz, the SE has up to about 70 dB. Compares Fig. 7a and 8a with Fig. 5a and 6a, we observe that there is another rapid increase even up to about 80dB at about 0.6 GHz for the electric field SE calculated at z = 25 cm because of boundary effect of the wall. The other obvious difference is that there are better electric field SE for the calculation points of z = 15 cm below 0.5 GHz in Fig. 7a and 8a, which indicates that the shape of aperture has some effect on the electric field SE at some calculation points for different polarization wave. In Fig. 8, there is fewer difference for the electric field SE of apertures located at y = 8 cm and y = 6 cm due to the aperture's different places, but for the SE of apertures located at y = 10 cm, it is absolutely different; the maximum of the difference is about 10 dB. For single aperture case, we can conclude that the electric field SE of enclosure is larger when the apertures are far from the center of the wall.

Multiple aperture case: In this section, we discuss electric field SE results calculated at three different points versus multiple apertures having different arrays of position. We also consider $30\times 12\times 30$ cm enclosure with rectangular apertures of size (4.0×4.0 cm and 2×2 cm). In Fig. 9, there are two 1.5×1.5 cm apertures located at array 1 ((150, 90, 0), (150, 30, 0)), array 2 ((200, 60, 0), (100, 60,0)), enclosure illuminated by vertical polarized plane wave. In Fig. 10, there are four 2×2 cm apertures located at array 1 ((130, 80, 0), (130, 40, 0), (170, 80, 0), (170, 40, 0)), array 4 ((240, 60, 0), (190, 60, 0), (110, 60, 0), (60, 60, 0)), array 5 ((150, 30, 0), (75, 30, 0), (240, 60, 0), (130, 80, 0)), enclosure also illuminated by vertical polarized plane wave. Compares the electric field SE in Fig. 9 and 10, we note that there are little difference for different arrays for multiple apertures, which demonstrate that aperture's location has little effect on the electric field SE.

CONCLUSION

In this study, an efficient evaluation approach based on modal MoM technique is presented to evaluate electric field SE of enclosures with multiple apertures at various places. Expressing electromagnetic fields in terms of cavity Green's function inside the enclosure and the free space Green's function outside the enclosure, integral equations with aperture tangential electric fields as unknown variables are obtained by enforcing the continuity of tangential electric and magnetic fields across the apertures. Using the Method of Moments, the integral equations are solved for unknown aperture fields. From these aperture fields, the electromagnetic fields inside a rectangular enclosure due to external electromagnetic sources are determined.

Numerical results on electric field SE of a rectangular enclosure with apertures are validated with data available in the literature and measurement. It is also shown that effect factors of electric field SE include calculation points, aperture' place, number and shape, polarization. Compared with single slit case, electric field SE of multiple apertures are less effected by apertures' position. The apertures' place have

different effects on the electric field SE of different calculation point and polarization. When the enclosure with apertures is illuminated by horizontal polarization plane wave, it has better electric field SE, especial for the aperture located at the center of wall. The electric field SE of enclosure is larger when the apertures are far from the center of the wall. And electric field SE near the aperture is lower than that at location inside the enclosure far away from the aperture below the resonance frequency. Therefore, single aperture should be located far from the center of the wall and low frequency sensitive apparatus inside the enclosure should be placed at the points far away from the apertures, which can improve the ability of electromagnetic compatibility. These useful results gained in this study have the important practical significance to improving the electric field SE of shielding cavity.

ACKNOWLEDGMENT

This study was supported by key program of National Science funds of China (No. U1233202), general program of National Science funds of China (No. 61179073), National Science funds of Civil Aviation Flight University of China (No. J2007-23) and Open Funds of CAAC academy of flight technology and safety.

REFERENCES

Ali, K.Z., C.F. Bunting and M.D. Deshpande, 2005. Shielding effectiveness of metallic enclosures at oblique and arbitrary polarizations. IEEE T. Electromagn. Compat., 47(1): 112-122.

Attari, R. and K. Barkeshli, 2002. Application of the transmission line matrix method to the calculation of the shielding effectiveness for metallic enclosures. Proceeding of the IEEE International Symposium on Antennas Propagation Society, 3: 302-305.

Bahadorzadeh, M. and M.N. Moghaddasi, 2008. Improving the shielding effectiveness of a rectangular metallic enclosure with aperture by using extra shielding wall. Progr. Electromagn. Res. Lett., 1: 45-50.

Belokour, D.W.P., J. LoVetri and S. Kashyap, 2001. A higher order mode transmission linemodel of the shielding effectiveness of enclosures with apertures. Proc. IEEE Int. Symp. Electromagn. Compat., 2(13-17): 702-707.

Benhassine, S., L. Pichon and W. Tabbara, 2002. An efficient finite-element time-domain method for the analysis of the coupling between wave and shielded enclosure. IEEE T. Magn., 38(2): 709-712.

Carpes, Jr. W.P., L. Pinchon and A. Razek, 2002. Analysis of the coupling of an incident wave with a wire inside a cavity using an FEM in frequency and time domains. IEEE T. Electromagn. Compat., 44(3): 470-475.

Dehkhoda, P., A. Tavakoli and R. Moini, 2009. Shielding effectiveness of a rectangular enclosure with finite wall thickness and rectangular apertures by the generalized modal method of moments. IET Sci. Meas. Technol., 3(2): 123-136.

Deshpande, M.D., 2000. Electromagnetic field Penetration Studies (NASA/CR-2000-210 297). Retrieved from: http://techre-orts.larc.nasa.gov/ltrs/PDF/2000/cr/NASA-2000-cr210 297.pdf.

Faghihi, F. and H. Heydari, 2009. Reduction of leakage magnetic field in electromagnetic systems based on active shielding concept verified by eigenvalue analysis. Progr. Electromagn. Res. (PIER), 96: 217-236.

Hussein, K.F.A., 2007. Effect of internal resonance on the radar cross section and shield effectiveness of open spherical enclosures. Progr. Electromagn. Res. (PIER), 70: 225-246.

Jayasree, P.V.Y., 2010. Analysis of shielding effectiveness of single, double and laminated shields for oblique incidence of EM waves. Progr. Electromagn. Res. B, 22: 187-202.

Jiao, C., X. Cui, L. Li and H. Li, 2006. Subcell FDTD analysis of shielding effectiveness of a thin-walled enclosure with an aperture. IEEE T. Magn., 42(4): 1075-1078.

Kim, Y.J., U. Choi and Y.S. Kim, 2008. Screen filter design consideration for plasma display panels (PDP) to achieve a high brightness with a minimal loss of EMI shielding effectiveness. J. Electromagn. Waves Appl., 22(5-6): 775-786(12).

Koledintseva, M.Y., J. Drewniak and R. DuBroff, 2009. Modeling of shielding composite materials and structures for microwave frequencies. Progr. Electromagn. Res. B, 15: 197-215.

Li, M., J. Nuebel, J.L. Drewniak, T.H. Hubing, R.E. DuBroff and T.P. Van Doren, 2000. EMI from cavity modes of shielding enclosures-FDTD modeling and measurements. IEEE T. Electromagn. Compat., 42(1): 29-38.

Morari, C., I. Balan, J. Pintea, E. Chitanu and I. Iordache, 2011. Electrical conductivity and electromagnetic shielding effectiveness of silicone rubber filled with ferrite and graphite powders. Progr. Electromagn. Res. M, 21: 93-104.

Podlozny, V., C. Christopoulos and J. Paul, 2002. Efficient description of fine features using digital filters in time domain computational electromagnetic. IET Sci. Meas. Technol., 149(5): 254-257.

Robertson, J., E.A. Parker, B. Sanz-Izquierdo and J.C. Batchelor, 2008. Electromagnetic coupling through arbitrary apertures in parallel conducting planes. Progr. Electromagn. Res. B, 8: 29-42.

Robinson, M.P., J.D. Turner, D.W.P. Thomas, J.F. Dawson, M.D. Ganley, A.C. Marvin, S.J. Porter, T.M. Benson and C. Christopolous, 1996. Shielding effectiveness of a rectangular enclosure with a rectangular aperture. Electron. Lett., 32(17).

Robinson, M.P., T.M. Benson, C. Christopoulos, J.F. Dawson, M.D. Ganley, A.C. Marvin, S.J. Porter and D.W.P. Thomas,1998. Analytical formulation for the shielding effectiveness of enclosures with apertures. IEEE T. Electromagn. Compat., 40(3): 240-248.

Thomas, D.W.P., A. Denton, T. Konefal, T.M. Benson, C. Christopoulos, J.F. Dawson, A.C. Marvin and J. Porter, 1999. Characterization of the shielding effectiveness of loaded equipment enclosures. Proceeding of the International Conference and Exhibition on Electromagnetic Compatibility. York, pp: 89-94.

Wallyn, W., D. De Zutter and H. Rogier, 2002. Prediction of the shielding and resonant behavior of multisection enclosures based on magnetic current modeling. IEEE T. Electromagn. Compat., 44(1): 130-138.

Wang, Y.J. and W.J. Koh, 2004. Coupling cross section and shielding effectiveness measurements on a coaxial cable by both mode-tuned reverberation chamber and Gtem cell methodologies. Progr. Electromagn. Res., 47: 61-73.

Wu, G., X.G. Zhang ad B. Liu, 2010. A hybrid method for predicting the shielding effectiveness of rectangular metallic enclosures with thickness apertures. J. Electromagn. Waves Appl., 24(8-9): 1157-1169(13).

Wu, G., X.G. Zhang, Z.Q. Song and B. Liu, 2011. Analysis on shielding performance of metallic rectangular cascaded enclosure with apertures. Progr. Electromagn. Res. Lett., 20: 185-195.